02,08

Electrodynamic modeling of a heterodyne mixer on a chip based on the Josephson HTS junction and a Vivaldi hybrid antenna

© E.A. Matrozovfa, A.V. Chiginev, L.S. Revin¶

Institute of Physics of Microstructures, Russian Academy of Sciences,
Nizhny Novgorod, Russia

¶ E-mail: rls@ipmras.ru

An electrodynamic simulation of a mixer system with a heterodyne based on a high-temperature superconducting (HTS) Josephson junction on a single chip has been performed. A new system design has been proposed as a mixer, combining a log-periodic antenna and a Vivaldi antenna, which has shown promising results in transmitting a reference signal for frequencies up to 125 GHz. The directivity and gain of the antenna at a frequency of 100 GHz were 6.51 and 6 dBi.

1. Introduction

High-temperature superconducting (HTSC) Josephson junctions have been increasingly used in recent years for development of high-frequency devices owing to their good sensitivity, high THz frequency limit, and the ability to operate at relatively high temperatures compared to devices based on low-temperature superconductors. The creation of a HTSC mixer based on the Josephson effect is one of the practically important objectives on [1–3]. The recent impressive results jcite4 are related to the measurement of noise temperature when mixing signals at a frequency of 600 GHz (900 K) and 1.5 THz (2500 K). At the same time, it is known that saturation of the HTSC mixer and deterioration of conversion efficiency take place with an increase of signal frequency and harmonic order. Therefore, an important task is to study the possibility of usage of a high-frequency reference signal source located on the same chip with the mixer.

Mixing with Josephson's intrinsic generation is possible in addition to mixing with an external heterodyne. Estimates of the line width of the intrinsic generation of low-resistance Josephson junctions YBaCuO provide values of the order of units of GHz and dozens of GHz for high-resistance junctions. The presence of such a wide line determines the use of intrinsic generation of HTSC junctions for studying the noise temperature and for analyzing broadband radiation. The use of external highly stable heterodyne sources with a line width of the order of kHz units makes it possible to study the spectral composition of the external signal. We consider in this paper the case of mixing with an external heterodyne based on a long Josephson junction, estimates of the line width of which give values of dozens of MHz.

A design of a monolithic HTSC mixer located entirely on a chip used with an external heterodyne, was proposed in Ref. [5]. Such a mixer demonstrated more efficient signal transmission due to the compactness of the proposed design and therefore lower losses, compared with mixers with spaced elements. We additionally propose to place a heterodyne source directly on the chip in this paper. This approach has a number of advantages compared to mixing a signal with an external heterodyne: compact size, low losses, low noise, which should have a positive effect on the characteristics of the mixer.

The concept of a superheterodyne mixer based on the superconductor-insulator-superconductor (SIS) transition has successfully proved itself in low-temperature superconducting technologies, where the reference signal source is a long Josephson junction located on the same chip with the receiver [9,10]. Mixing systems are based on the tunneling of quasiparticles through a barrier located between two superconductors, while their frequency is fundamentally limited by the energy gap in superconducting niobium. However, higher slot energy SIS transitions have been recently developed to expand the frequency range. Unlike SIS mixers, Josephson HTSC mixers use the nonlinearity of the Cooper pair current. In addition to the apparent advantage of a much higher operating temperature, their higher energy slot results in a cutoff frequency of several THz. The Josephson effect, realized in the usage of HTSC junctions, allows not only sensitive reception of an external signal, but also generation of GHz and sub-THz frequency range signals [6–8].

The implementation of an HTSC receiver, similar to a low-temperature SIS receiver, is associated with certain technological constraints. High-temperature Josephson junctions formed either at the boundary of a bicrystalline

substrate or by ion irradiation, unlike niobium junctions, are single-layer structures. Therefore, it is not possible to realize the transmission of a high-frequency signal over a microstrip line using this technology. Nevertheless, studies of the Josephson HTSC signal source on the chip are actively underway [11–13].

The Josephson HTSC mixer can be excited by a heterodyne source using various methods: a coplanar line, near-field interaction, and a Vivaldi antenna.

It is possible to transmit a signal only in a narrow frequency range up to 50 GHz when using a coplanar line [3]. The signal transmitted along the coplanar line is radiated into the surrounding space at higher frequencies until it reaches the Josephson junction.

The excitation of the mixer by the near-field interaction [11] can be performed by placing the Josephson junction in the center of the log-periodic antenna [14,15] and placing it near the dipole antenna. At the same time, the dipole can be shaped as a line repeating the edge of the log-periodic antenna to increase the capacitive coupling. A critical disadvantage of such a system is the weakness of the near-field interaction because of the small end areas of the structures forming the walls of the „capacitor". At the same time, the edge effects of the propagation of electromagnetic fields begin to play an important role in the interaction of structures. The weakness and narrow-band of the near-field interaction significantly limits the possibility of its application to excite a Josephson mixer.

The use of the Vivaldi antenna can be a promising alternative method for implementation of a mixer on a chip [16]. Vivaldi antenna is an ultra-wide-band emitter built on the basis of an expanding slot line. The Josephson junction is assumed to be used as a nonlinear element. The Vivaldi antenna has a high directivity and emits mainly in the direction of the open end of the slot along the axis of symmetry, creating a symmetrical beam in the E- and H-planes. The reciprocity of the antenna design allows it to be used both as a transmitter and as a receiver. Such an antenna has a simple geometry, is easy to manufacture, but at the same time it is effective.

The proposed new mixer design, combining a Vivaldi antenna with a log-periodic antenna, can allow mixing on a single chip: the external signal is received perpendicular to the structure using a log-periodic antenna, whereas the reference signal propagates along the substrate emitted by the Vivaldi antenna.

2. Electrodynamic modeling of the system

The Vivaldi antenna is an exponentially expanding slot that begins with a uniform slot line and gradually expands to a width of about $\lambda_{\text{eff}}/2$, where λ_{eff} — the wavelength in the medium. The electric field is gradually converted from the slot mode to the radiation mode owing to such design and is finally emitted when the distance between the two
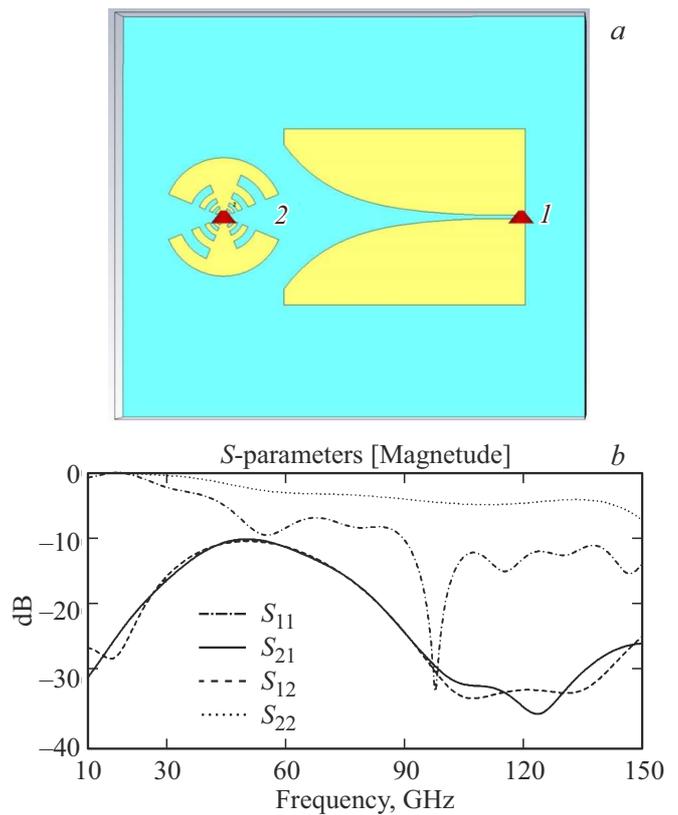
Figure 1. Superheterodyne receiver design. a) Port 1 — Josephson reference signal generator integrated into the Vivaldi antenna. Port 2 — Josephson mixer integrated into a log-periodic antenna. b) S-parameters in case of the excitation of the log periodic antenna using the Vivaldi antenna.

arms of the antenna reaches $\sim \lambda_{\text{eff}}/2$. Thus, the upper and lower frequency limits are determined by the width of the antenna slot on the supply and radiating sides, respectively. The dimensions of the subject Vivaldi antenna (Figure 1, a) were: width — $880.3\,\mu$m, length — $1200\,\mu$m, width of the slot in the radiating section — $720\,\mu$m, the width of the slot in the supply section — $19.2\,\mu$m.

The directional pattern (DP) of the Vivaldi antenna beam is determined by the size of the antenna, the exponential law of opening the slot line, as well as the thickness and material of the substrate (dielectric constant) [17]. The bottom in the H plane depends on the phase velocity of the directional wave and the length of the antenna, and the bottom in the E plane also depends on the shape of the slot cone [18]. It is necessary to control the phase velocity of the directed wave for obtaining the desired DP, i.e. by changing the width/shape of the cone or by changing the substrate material used (dielectric constant ε, thickness d). The beam width narrows and the gain increases as the antenna length increases in case of the Vivaldi antenna, as in case of other surface wave antennas [19].

When selecting the substrate material and its thickness, it is convenient to be guided by an empirical assessment

linking the characteristics of the substrate with the formation of the antenna bottom on surface waves [19,20]. According to this assessment, the correct selection of substrate parameters allows obtaining optimal directional pattern. This is due to the impact of the dielectric constant ε and the thickness of the substrate d on the phase velocity of the directed wave. The main lobe of the bottom splits and the side lobes increase if the upper limit of the optimal range of values is exceeded d ($\varepsilon^{-0.5} - 1$). In the case of values less than the lower limit of the optimal range, the gain and side lobes of the directional pattern decrease. It follows from these estimates that the preference should be given to the thinnest substrates with the lowest dielectric constant when operating at high frequencies of the order of tens and hundreds of GHz. In our case, for the Vivaldi antenna (Figure 1, a), when using an MgO substrate ($\varepsilon = 9.63$) with a thickness of $500 \mu m$ at a frequency of $200 \, GHz$, the gain directional pattern has a main lobe directed along the central axis of the antenna with an amplitude of $-92.9 \, dBi$, whereas in case of usage of the cubic zirconia ($\varepsilon = 24$) of the same thickness, the main lobe splits into two, and a dip of the directional pattern is formed on the axis of symmetry. If it is necessary to work with substrates with a high dielectric constant, possible solution may include either a significant reduction of the thickness of the substrate or the use of an additional dielectric layer located on top of the entire structure with the exception of the transition regions [21]. Further modeling was performed on MgO substrates.

It is proposed to use a log-periodic antenna [22,23] as a mixer with a nonlinear element — Josephson junction placed in its center. The log periodic antenna has a planar geometry, it is broadband, and emits in a plane perpendicular to the antenna plane. The lengths of the minimum and maximum lobes of the antenna determine the frequency range of its radiation. We consider in this paper a log antenna designed for the frequency range of $50-800 \, GHz$ [24] with an outer diameter of $592.3 \, \mu m$.

The issue of alignment with the antenna system plays a critical role in the use of Josephson junction HTSC for practical applications. A number of experimental studies demonstrated that YBaCuO junctions have a low resistance of the order of units Ω [25–29]. The solution to this problem can be the use of chains or arrays of Josephson junctions [24] or the use of high-resistance HTSC junctions with a resistance of the order of several dozens Ω [1,4]. The impedance of the port simulating the Josephson junction was $50 \, \Omega$ in the completed simulation, which corresponds to the differential resistance of the HTSC mixer at the operating point.

The first variant of implementing a receiver with a heterodyne on a chip was combining a Vivaldi antenna and a log-periodic antenna (Figure 1, a). The Josephson HTSC junction, acting as a nonlinear element, was located in the center of the log-periodic antenna, the reference signal of the Josephson generator was emitted using a Vivaldi antenna.

The finite difference method was used as a numerical method for the simulation. Calculations were performed
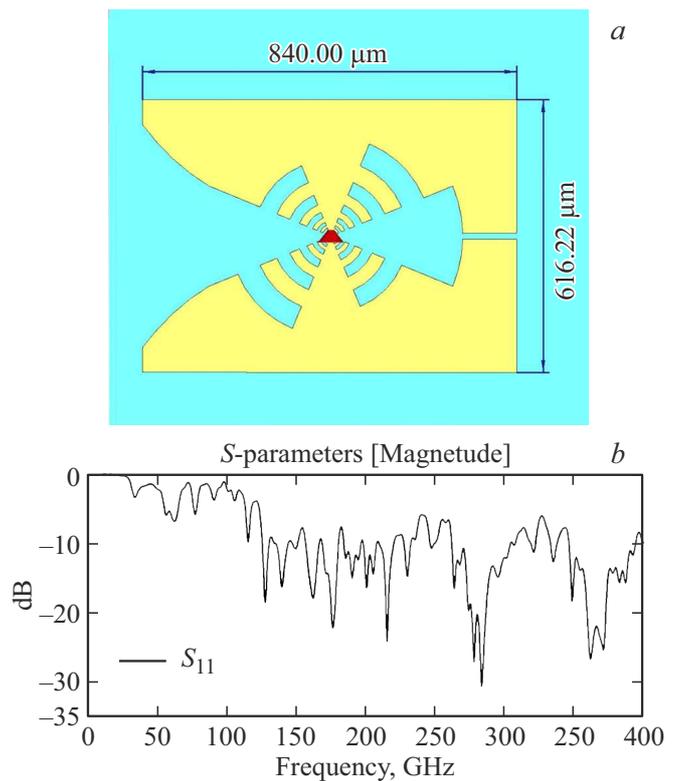
Figure 2. Hybrid antenna. a) Hybrid antenna design. b) S-parameters of the hybrid antenna.

in the time domain in the frequency range from 10 to $400 \, GHz$. Discrete ports 1 and 2 were used for excitation of the system. Port 1, simulating the source of the heterodyne, was located between the electrodes of the Vivaldi antenna, port 2 (mixer) was located between the electrodes of the log periodic antenna in its center, at the place of the Josephson HTSC junction. The scattering matrix (S-parameters) of the system were calculated during simulation. Software monitors of fields in the far zone at frequencies from 100 to $400 \, GHz$, inclusive, in increments of $100 \, GHz$ were used to model the directional patterns. The boundary conditions above the substrate were defined as open with added space; the boundary conditions are open in all other directions.

Figure 1, b shows S-parameters for this system. The chart shows that signal transmission is possible in the range from 30 to $70 \, GHz$, while S12 is approximately at the level of $-15 \, dB$. This significant signal suppression is explained by the specific features of the antennas used: the reference signal of the Vivaldi antenna is radiated along the substrate, however, the receiving log-periodic antenna receives the main part of the signal perpendicular to the substrate.

It was proposed to use a new hybrid antenna variant to solve the problem of poor signal transmission wherein the Vivaldi antenna and the log-periodic antenna are combined (Figure 2, a). The antenna width was $616.2 \, \mu m$, length — $840 \, \mu m$, antenna opening width — $504 \, \mu m$. The hybrid antenna was located on a silicon lens with a radius of
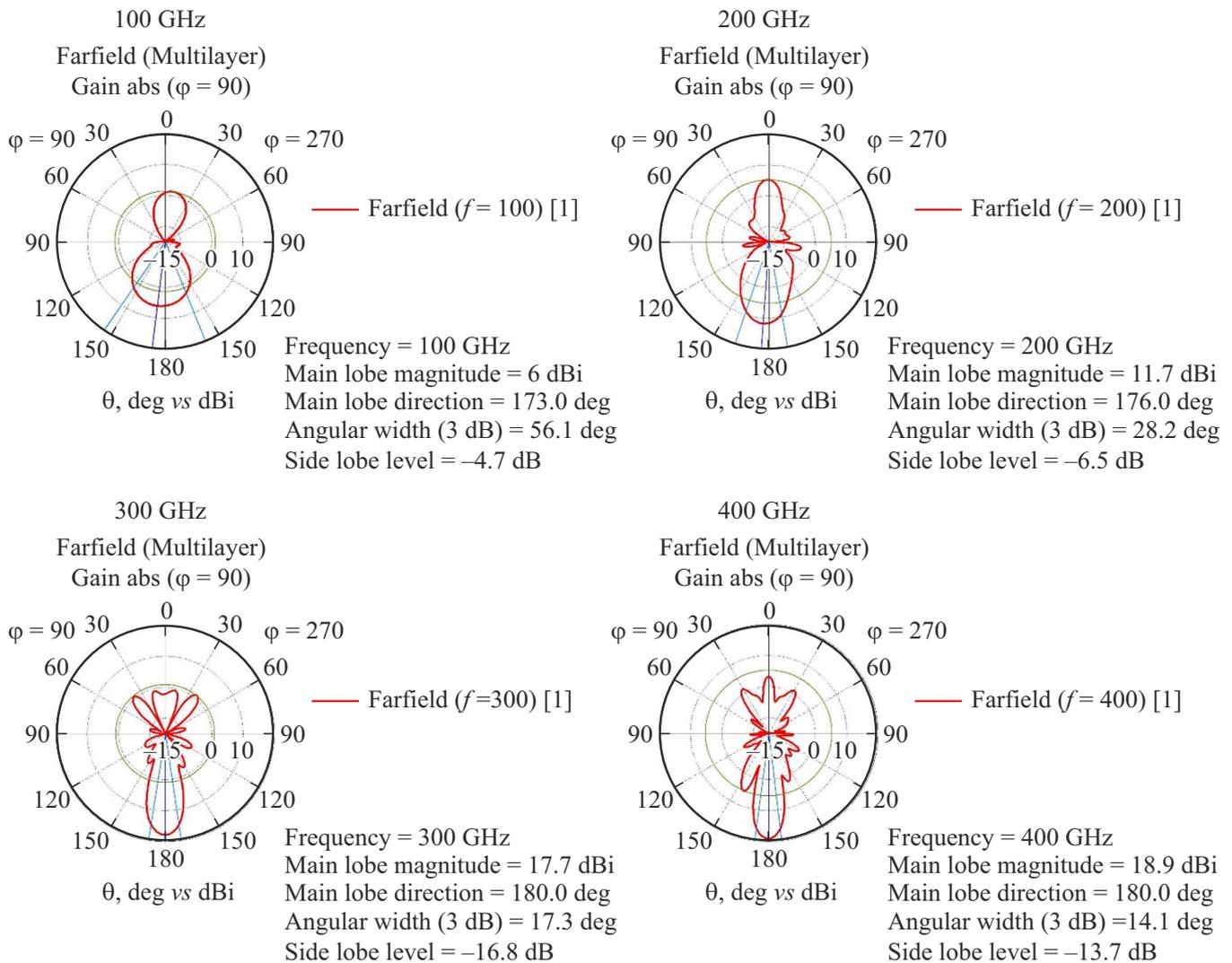
Figure 3. Directional patterns of the hybrid antenna for frequencies of 100, 200, 300 and 400 GHz.

1.5 mm during simulation. *S*-parameter of the hybrid antenna is shown in Figure 2, *b*. The figure shows that this antenna is broadband and emits/receives well at frequencies from 110 GHz.

The names of the hybrid antenna for frequencies $f = 100, 200, 300$ and 400 GHz are shown in Figure 3. The directivity and gain of the antenna were 6.51 dBi and 6 dBi at a frequency of 100 GHz, 12.3 dBi and 11.7 dBi at a frequency of 200 GHz, 18.1 dBi and 17.7 dBi at a frequency of 300 GHz, 19.1 dBi and 18.9 dBi at a frequency of 400 GHz, respectively. As can be seen from the charts, the width of the main lobe of the DP narrows, the directivity and gain of the antenna increase with the increase of the frequency.

Figure 4, *a* shows the mixer design based on a hybrid antenna and a Vivaldi antenna. The dimensions of the hybrid antenna correspond to those shown in Figure 2. The general scheme of the Josephson HTSC mixer is shown in Figure 4, *b*. The structure is located on an MgO substrate;

a silicon lens is located on the reverse side of the substrate. The external RF signal is transmitted from the lens side and is received by a hybrid antenna. The reference signal of the heterodyne is controlled by supplying a direct bias current to the Josephson bicrystalline junction located in the opening of the Vivaldi antenna. The external high-frequency signal is mixed with the signal from the heterodyne at the Josephson junction located in the center of the hybrid antenna. The output signal is read at an intermediate frequency from a hybrid antenna.

Figure 5 shows the *S*-parameters of the resulting system. It can be seen that signal transmission is possible in the band from 50 to 125 GHz, while S_{12} corresponds to a value of approximately -15 dB, which exceeds the operating frequency range obtained for a system with a standard log-periodic antenna. It should be noted that the use of high-resistance Josephson transitions in this case plays a key role: for example, the transition from 50- to 5 Ω-Josephson junctions leads to suppression of S_{12}
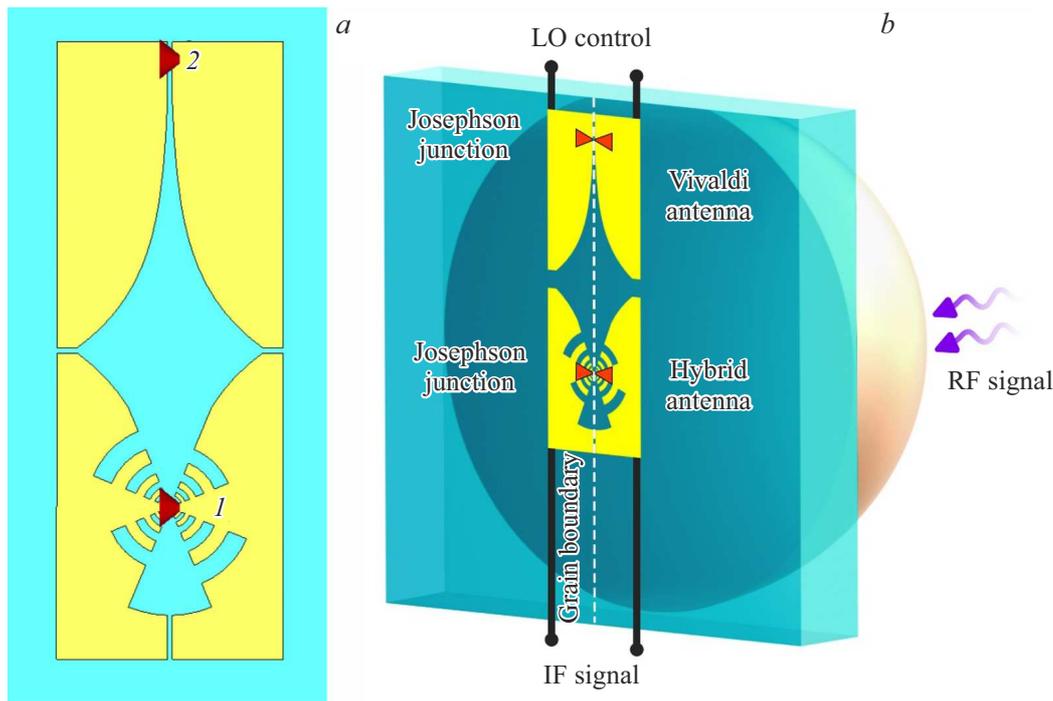
Figure 4. Mixer design with hybrid antenna. *a*) View from above. *b*) The scheme of the Josephson HTSC mixer: Josephson junction – Josephson junction; Grain boundary — bicrystalline boundary on the MgO crystal; LO Control — Direct current displacement control of the Josephson junction located in the Vivaldi antenna opening; RF Signal — External high-frequency signal; IF Signal — intermediate frequency output signal.
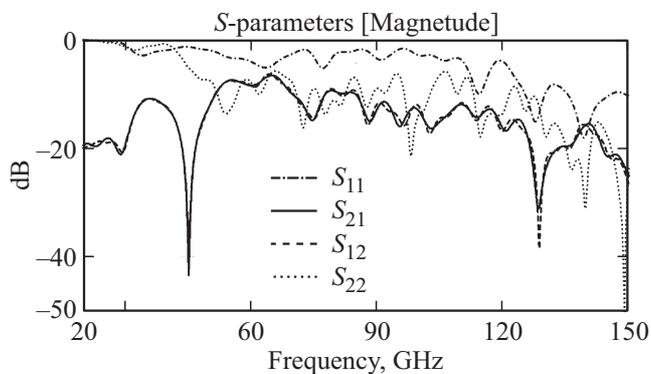
Figure 5. *S*-parameters in case of excitation of a hybrid antenna using a Vivaldi antenna.

by values of the order of 10 dB in the frequency range 50−150 GHz.

3. Conclusion

It was found as a result of electrodynamic simulation that the creation of a mixer located entirely on a chip using the Josephson HTSC junction is possible by the use of a new hybrid antenna type combining a log-periodic antenna and a Vivaldi antenna. Signals can be transmitted in such systems up to frequencies of the order of 125 GHz.

The directivity and gain of the antenna at a frequency of 100 GHz were 6.51 dBi and 6 dBi, respectively, the parameter S_{12} corresponds to a value of the order −15 dB.

There are many methods to modify the Vivaldi antenna to improve its gain and directional pattern. Additional elliptical elements located on the sides of the Vivaldi antenna are used Ref. [30] to increase the antenna gain. In a number of papers such as [31,32] the improvement of the radiating properties of the antenna is achieved through the use of additional planar resonators in the form of crosses, arrows, squares and other geometric shapes, as well as rectangular slots cut out on the sides of the Vivaldi antenna. The use of an additional dielectric resonator is proposed in Ref. [33]. The use of Vivaldi antenna design modifications to create a mixer on a chip seems promising and requires further studies.

Funding

Conflict of interest

The authors declare that they have no conflict of interest.

References

[1] H. Shimakage, Y. Uzawa, M. Tonouchi, Z. Wang. IEEE Trans. Appl. Supercond. **7**, *2*, 2595 (1997).

[2] M. Malnou, C. Feuillet-Palma, C. Ulysse, G. Faini, P. Febvre, M. Sirena, L. Olanier, J. Lesueur, N. Bergeal. J. Appl. Phys. **116**, *7*, 074505 (2014).

[3] X. Gao, T. Zhang, J. Du, A.R. Weily, Y.J. Guo, C.P. Foley. Supercond. Sci. Technol. **30**, *9*, 095011 (2017).

[4] D. Cunnane, J.H. Kawamura, N. Acharya, M.A. Wolak, X.X. Xi, B.S. Karasik. Appl. Phys. Rev. **109**, *11*, 112602 (2016).

[5] X. Gao, T. Zhang, J. Du, Y.J. Guo. Supercond. Sci. Technol., **31**, 115010 (2018).

[6] V.P. Koshelets, P.N. Dmitriev, A.B. Ermakov, A.S. Sobolev, A.M. Baryshev, P.R. Wesselius, J. Mygind. Supercond. Sci. Technol. **14**, *12*, 1040 (2001).

[7] M.A. Galin, A.M. Klushin, V.V. Kurin, S.V. Seliverstov, M.I. Finkel, G.N. Goltsman, F. Müller, T. Scheller, A.D. Semenov. Supercond. Sci. Technol. **28**, *5*, 055002 (2015).

[8] L.S. Revin, D.V. Masterov, A.E. Parafin, S.A. Pavlov, D.A. Pimanov, A.V. Chiginev, A.V. Blagodatkin, I.V. Rakut', E.V. Skorokhodov, A.V. Gordeeva, A.L. Pankratov. Appl. Sci. **12**, *23*, 11960 (2022).

[9] V.P. Koshelets, S.V. Shitov. Supercond. Sci. Technol. **13**, *5*, R53 (2000).

[10] V.P. Koshelets, S.V. Shitov, A.V. Shchukin, L.V. Filippenko, J. Mygind, A.V. Ustinov. Phys. Rev. B **56**, *9*, 5572 (1997).

[11] B. Chesca, D. John, M. Gaifullin, J. Cox, A. Murphy, S. Savel'ev, C.J. Mellor. Appl. Phys. Lett. **117**, *14*, 142601 (2020).

[12] M. Darula, T. Doderer, S. Beuven. Supercond. Sci. Technol. **12**, *1*, R1 (1999).

[13] K. Lee, I. Iguchi, K.Y. Constantinian. Physica C **320**, *1−2*, 65 (1999).

[14] H. Saijo, M. Morimoto, M. Yamashita, M. Tonouchi, M. Hangyo. Technical Digest. CLEO/Pacific Rim'99 (Cat. No. 99TH8464) **2**, 451 (1999).

[15] M. Tonouchi, H. Saijo, M. Hangyo, O. Morikawa, P. Gu, M. Tani, K. Sakai. Physica C **357−360**, *Part 2*, 1600 (2001).

[16] P.J. Gibson. 9th Eur. Microwave Conf. Proceed. **101** (1979).

[17] P. Ludlow, V. Fusco. In: 2009 Loughborough Antennas & Propagation Conf. (IEEE) (2009). 445 p.

[18] R. Janaswamy, D.H. Schaubert. IEEE Trans. AP **35**, *9*, 1058 (1987).

[19] K.S. Yngvesson, T.L. Korzeniowski, Y.-S. Kim, E.L. Kollberg, J.F. Johansson. IEEE Trans. Microwave Theory. Techniques **37**, *2*, 365 (1989).

[20] N. Tiwari, T.R. Rao. ACES J. **32**, *4*, 366 (2017).

[21] M.F. Abdullah, A.K. Mukherjee, R. Kumar, S. Preu. J. Infrared Milli Terahz Waves **41**, *6*, 728 (2020).

[22] M.M. Gitin, F.W. Wise, G. Arjavalingam, Y. Pastol, R.C. Compton. IEEE Trans. Antennas Propag. **42**, *3*, 335 (1994).

[23] Y. Huo, G.W. Taylor, R. Bansal. Int. J. Infrared Millimeter Waves **23**, *6*, 819 (2002).

[24] E.I. Glushkov, A.V. Chiginev, L.S. Kuzmin, L.S. Revin. Beilstein J. Nanotechnol. **13**, 325 (2022).

[25] C. Pegrum, T. Zhang, J. Du, Y.J. Guo. IEEE Trans. Appl. Supercond. **26**, *3*, 1500905 (2016).

[26] X. Gao, H. Li, T. Zhang, J. Du, K. Smart, J. Ma, J. An. Opt. Express **30**, *20*, 35311 (2022).

[27] X. Gao, T. Zhang, J. Du, Y.J. Guo. IEEE Trans. Terahertz Sci. Technol. **10**, *1*, 21 (2020).

[28] X. Gao, H. Li, J. Song, J. An, X. Bu, H. Liu. J. Appl. Phys. **130**, *17*, 173903 (2021).

[29] J. Du, C.M. Pegrum, X. Gao, A.R. Weily, T. Zhang, Y.J. Guo, C.P. Foley. IEEE Trans. Appl. Supercond. **27**, *4*, 1500905 (2017).

[30] S. Poorgholam-Khanjari, F.B. Zarrabi. Opt. Commun. **480**, 126482 (2021).

[31] R.K. Kushwaha, P. Karuppanan. Opt. Quant. Electron. **51**, *9*, 309 (2019).

[32] O. Turkmen-Kucuksari, A. Kocakaya, S. Çimen, G. Çakır. AEU — Int. J. Electron. Commun. **113**, 152975 (2020).

[33] J. Bourqui, M. Okoniewski, E.C. Fear. IEEE Trans. AP **58**, *7*, 2318 (2010).

Translated by A.Akhtyamov